Deep-Sea Research II ▮ (▮▮▮▮) ▮▮▮–▮▮▮

Contents lists available at SciVerse ScienceDirect

Deep-Sea Research II

journal homepage: www.elsevier.com/locate/dsr2

Roles of sorption and tube-dwelling benthos in the cycling of phosphorus in Bering Sea sediments

Emily S. Davenport [a,*,1], David H. Shull [a,2], Allan H. Devol [b,3]

[a] Department of Environmental Sciences, Huxley College of the Environment, Western Washington University, 516 High Street, Bellingham, WA 98225, USA
[b] University of Washington, School of Oceanography, Seattle, WA 98195, USA

ARTICLE INFO

Keywords:
USA
Alaska
Bering Sea
Adsorption
Benthos
Climate change
Continental shelves
Phosphorus cycle

ABSTRACT

Adsorption of dissolved phosphate onto iron-hydroxides has been shown to be one of the primary regulators of phosphorus cycling in sediments. Bioturbation and bioirrigation by benthic infauna modify this cycling by accelerating the transport of dissolved and particulate phosphorus and by changing rates of reactions that occur in the sediment, such as the adsorption of phosphate by amorphous iron hydroxides. Hydrographic processes vary regionally in the Bering Sea and nutrient exchange between the sediments of the broad shallow shelf and overlying water may influence water column productivity. These characteristics make the Bering Sea a good study site for examining the processes that influence sedimentary cycling of phosphorus. To examine these processes, we collected samples in four domains (southern middle shelf, southern outer shelf, southern off shelf (consisting of the continental slope and Bering Sea basin) and northern Bering shelf) based on hydrographic regime. At each station we directly measured phosphate flux and sediment oxygen consumption using whole–core incubations. We also measured infaunal burrow abundances, amorphous iron-hydroxide concentrations and phosphate sorption. We found that three out of the four domains had a high affinity for trapping phosphate in the sediment, as indicated by their adsorption coefficients (6.59–81.81). However, the measured phosphate fluxes could not be explained by the adsorption capacity of the sediment alone. The results indicated that on the middle shelf, the phosphate flux positively co-varied with infaunal burrow abundances. The high number of organisms in this domain (10–32 burrows per 50 cm^2 core) enhances the flux of phosphate to the overlying water. Controls on the phosphate flux on the middle shelf cannot be properly understood unless benthic infaunal abundance is taken into account.

1. Introduction

1.1. The phosphorus cycle

Sediments represent the largest reservoir of phosphorus on earth and processes controlling phosphorus cycling in sediments are complex (Burdige, 2006; McManus et al., 1997; Van Capellen and Ingall, 1994). Continental margin sediments are important sinks for carbon, nitrogen and phosphorus. Because phosphorus is thought to limit oceanic primary production on long time scales (e.g., Redfield, 1958; Schlesinger, 2004; Schulz and Zabel, 2006; Tyrrell, 1999) and may constrain productivity in the coastal ocean (Palenik and Dyhrman, 1998) it is important to understand the various processes that control the cycling of this biologically reactive element between sediments and the overlying water.

Unlike nitrogen, phosphorus does not have a gaseous phase. The primary source of biologically available dissolved phosphorus, in the form of phosphate, is the weathering of continental rocks, which delivers phosphorous to the oceans through riverine input (Schulz and Zabel, 2006; Tyrrell, 1999). Burial of phosphorus as authigenic apatite in continental shelf sediments is the only significant loss of phosphorus from the oceans (Burdige, 2006; Froelich, 1988; Schlesinger, 2004; Sundby et al., 1992).

The decomposition of organic matter at the sediment surface causes the release of dissolved phosphate to the sediment pore water, which may then be released to the overlying water, re-precipitated as authigenic apatite, or adsorbed to sediment particles (Anschutz et al., 1998). In the oxidized layer of the sediment, adsorption to iron-hydroxides has been shown to be

* Corresponding author. Tel.: +1 360 556 5376.
E-mail addresses: davene@uga.edu (E.S. Davenport), david.shull@wwu.edu (D.H. Shull), devol@u.washington.edu (A.H. Devol).
[1] Present address: University of Georgia, Department of Marine Sciences, 220 Marine Sciences Building, Athens, GA 30602. USA. Tel.: +1 706 542 2915; fax: +1 706 542 3652.
[2] Tel.: +1 360 650 3690.
[3] Tel.: +1 206 685 3351.

0967-0645/$ - see front matter © 2012 Elsevier Ltd. All rights reserved.
doi:10.1016/j.dsr2.2012.02.004

one of the principal sorption reactions involving phosphate (Schulz and Zabel, 2006). Adsorption results in a buffering of the pore-water dissolved phosphate concentrations, maintaining relatively low values in solution, thereby limiting the flux of phosphate to the overlying water (Froelich, 1988; Slomp et al., 1998; Sundby et al., 1992). Within deeper, reduced sediment, iron-hydroxides undergo reduction and phosphate is released back to solution. Iron-hydroxide-bound phosphorus in surficial sediments is transported to deeper reduced sediments through sedimentation and bioturbation.

Mechanisms controlling phosphorus exchange between the sediments and overlying water vary in different regions. For example, in Rehoboth Bay (Delaware), seasonal variation in iron redox chemistry controls phosphate flux (Rozan et al., 2002). In the eastern South Atlantic, the highest release of phosphate came from sediments near coastal upwelling zones (Zabel et al., 1998). In the western North Pacific, bottom-water dissolved oxygen exerted a control on phosphate flux (McManus et al., 1997). These observations led us to ask what processes control phosphorus cycling in sediments from the Bering Sea, a region with a broad continental shelf and considerable variation in hydrography and primary productivity (Stabeno et al., 2001; Stabeno et al., this issue; Hunt et al., 2002).

1.2. Role of the benthos in the phosphorus cycle

Benthic infauna are often the dominant agents of particle and fluid transport and play a key role in sediment decomposition reactions and nutrient regeneration (Aller, 1978, 1982; Waldbusser et al., 2004). Benthic infauna burrows permeate the sediment. Through their feeding and burrow-construction activities, they disturb the sediment and can move iron-hydroxide particles from the oxidized to the reduced zone of the sediment. This transport causes iron-hydroxides to undergo reduction, releasing iron-bound phosphate to the pore water. Organisms can also aid in the re-oxidation of reduced iron by moving it from the reduced to oxic zone. Burrow ventilation brings oxygenated overlying water that is low in dissolved phosphate (relative to pore water) down into burrows, where a portion of this water can be exchanged with the surrounding sediment pore water. Phosphate dissolved in the water is then biologically transported from depth in the sediment to the overlying water column through burrow ventilation, and can by-pass the sorptive amorphous iron-hydroxides in oxidized surficial sediments (Aller, 1978, 1982). Organism abundance and activity are not always accounted for in conventional flux and pore-water diffusion models. Activities in the sediment alter the rate and geometry of pore-water transport, which can directly affect the rate of exchange of dissolved phosphate with overlying water. Consequently, phosphate fluxes in sediments possessing a highly sorptive surface layer might be strongly affected by the presence of ventilated infaunal burrows.

1.3. Study area

This study was part of a multidisciplinary expedition to the Bering Sea, the Bering Ecosystem Study (BEST). A research cruise aboard the USCGC Healy (WAGB 20) took place at the beginning of the spring ice retreat, from March 30th to May 6th, 2008. Seventeen stations were sampled along depth, productivity, latitude and distance (from shore) gradients (Fig. 1).

The Bering Sea shelf is wide (500 km), shallow and contains 3% of the world's continental shelf (Goering and Iverson, 1981; Hunt et al., 2002). The shelf area can be divided into four different domains: southern outer, middle, coastal (inner) shelf and northern Bering shelf, each characterized by a unique hydrographic structure as well as variation in primary production, nutrient

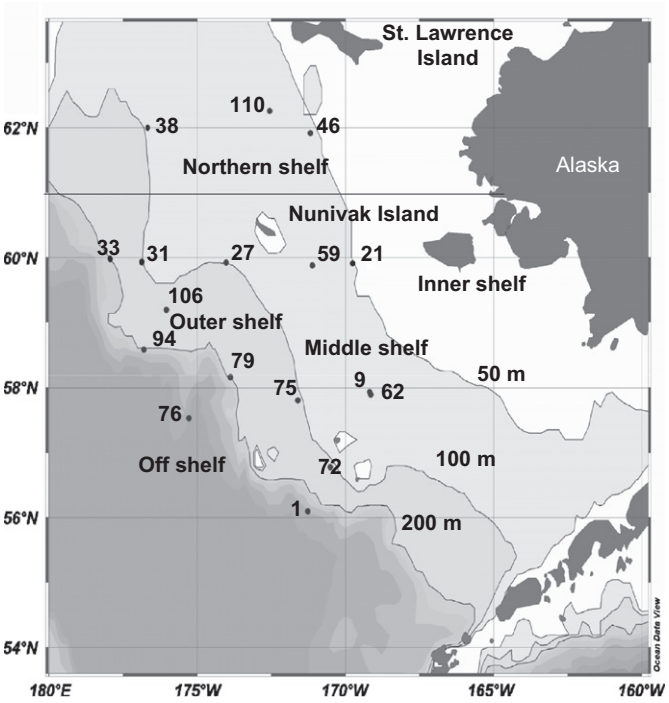

Fig. 1. Sampling locations in the Bering Sea. The bathymetry lines indicate the locations of the different fronts that form on the continental shelf, as defined in Hunt et al., 2002. These fronts form the seaward boundaries for the middle shelf and outer shelf domains. Beyond the 200 m isobath lies the continental slope and Bering Sea basin (off shelf domain). North of Nunivak Island (approximated by horizontal line) is the northern shelf domain. Map created using Ocean Data View (Schlitzer, 2008).

input and food-web organization (Coachman, 1986; Hunt et al., 2002; Stabeno et al., 2001, Stabeno et al., this issue). On the southern shelf, three distinct oceanographic fronts form after the spring ice retreat that separate it into three domains—coastal, middle and outer shelf (Goering and Iverson, 1981; Hunt et al., 2002; Lomas et al., this issue; Schumacher et al., 1979). The northern Bering shelf exists north of St. Matthew and Nunivak Islands (61°N latitude) and is relatively shallow (around 50 m) compared to the rest of the Bering Sea shelf (Hunt et al., 2002). Beyond the 200 m isobath lies the off shelf domain, consisting of the continental slope and Bering Sea basin (Fig. 1).

Productivity is generally greater at the outer shelf stations, where a substantial amount of upwelling occurs, compared to the middle and inner shelf domains (Hunt et al., 2002; Springer et al., 1996). Also, the melting sea ice may provide a source of dissolved iron to this domain that helps support ice-edge phytoplankton blooms (Aguilar-Islas et al., 2008). The inner and middle shelf domains may receive greater year-round input of iron and phosphorus derived from non-organic matter sources, such as continental weathering, than the outer shelf domains (Burdige, 2006; Schlesinger, 2004).

1.4. Significance

Little is known about the sedimentary Bering Sea phosphorus cycle. While the Bering shelf accounts for approximately 3% of the total area of the global continental shelf, the Arctic and adjacent continental shelf regions including the Bering Sea account for 25% of the global continental shelf area. Thus, measurements of the rates of phosphate flux (and the factors affecting this flux) in the Bering Sea could provide better constraints on the global phosphorus cycle. Since nitrogen to phosphorus ratios are used by researchers to assess sources and sinks of nitrogen in the

Please cite this article as: Davenport, E.S., et al., Roles of sorption and tube-dwelling benthos in the cycling of phosphorus in Bering Sea sediments. Deep-Sea Res. II (2012), doi:10.1016/j.dsr2.2012.02.004

Bering Sea, (e.g., Lehmann et al., 2005; Tanaka et al., 2004) better quantification of the phosphate cycle could also improve our understanding of the Bering Sea nitrogen cycle.

2. Methods

2.1. Shipboard analyses

At each station, up to 16 core samples were collected using an Ocean Instruments MC-800 eight-tube multi-corer, which takes 10 cm diameter cores up to 40 cm in length while preserving the sediment–water interface. Bottom water was also collected at each station using a Niskin bottle attached to the multi-corer.

2.1.1. Diffusive fluxes

If molecular diffusion were the dominant transport process occurring in sediments, the flux of solutes could be calculated directly from a profile of dissolved solute concentrations in the sediment using Fick's first law of diffusion. To determine profiles of dissolved phosphate, two cores per station were sectioned at 0.5 cm intervals to 2 cm and then 1 cm intervals to 20 cm or to the bottom of the core. The sediment from each depth was placed into a 50 ml centrifuge tube and centrifuged at 10,000 rpm to separate pore water from the solid phase. Pore water was then filtered in a nitrogen glove bag using 0.45 μm syringe filters and analyzed for dissolved reactive phosphate. Phosphate concentrations were determined colorimetrically using a modification of the EPA protocol 365.1. Sodium dodecyl sulfate was used as the surfactant, ammonium molybdate and antimony potassium tartrate in 2M sulfuric acid solution were the main reactants and ascorbic acid was used as the reductant. The samples were analyzed on a SmartChem autoanalyzer (Westco Scientific) at a wavelength of 880 nm. Phosphate diffusive fluxes were determined from the sediment phosphate profiles using Fick's first law of diffusion, $J=-\varphi D' dC/dz|_{z=0}$, where J is the flux in $\mu mol\ m^{-2}\ d^{-1}$, φ is the sediment porosity, D' is a diffusion coefficient ($cm^2\ s^{-1}$) corrected for tortuosity ($D'=D_m/\theta^2$, where D_m is the temperature-corrected molecular diffusion coefficient for phosphate and θ the sediment tortuosity is approximated by the empirical formula $\theta^2=1-\ln(\varphi^2)$; Boudreau, 1997), $dC/dz|_{z=0}$ is the concentration gradient at the sediment surface, and the negative sign indicates the direction of the flux is down the concentration gradient.

2.1.2. Phosphate adsorption experiments

To determine the importance of phosphorus sorption onto sediment particles, we performed adsorption experiments using surface sediments collected at each station. The top 3 cm of one sediment core from each station was removed and homogenized. Three centimeters was chosen as the depth because nitrate profiles collected from the same stations often extended to 3 cm, indicating the depth at which iron reduction begins (Burdige, 2006). Twenty milliliters of this sediment was placed into 50 ml centrifuge tubes with 20 ml of low-nutrient seawater (surface seawater from the equatorial Pacific Ocean) spiked with a known concentration of phosphate (0, 10, 20, 30, 40, or 50 μM). The P-spiked seawater was not deoxygenated prior to addition to centrifuge tubes in order to simulate redox conditions of surficial sediment. Phosphate concentrations of the P-spiked seawater were determined colorimetrically as a molybdenum-blue complex on a Technicon Autoanalyzer II (Mordy et al., 2005). The centrifuge tubes were capped and allowed to shake on a shaker table at in-situ temperatures (± 2 °C). After 24 h, the tubes were centrifuged at 10,000 rpm for 20 min, the supernatant was filtered using 0.45 μm syringe filters and the amount of phosphate remaining in solution at the end of the experiment was analyzed for dissolved reactive phosphate colorimetrically on the SmartChem autoanalyzer as described previously.

Total dissolved phosphate in each centrifuge tube at the beginning of the experiment was calculated using the average pore-water phosphate concentration in the top 3 cm and the average porosity over the top 3 cm. The concentration of dissolved phosphate remaining in solution at the end of the experiment was measured. To calculate the mass of phosphate adsorbed during the experiment (per gram of dry sediment) the equation $C^*=((C_{initial}-C_{final})(V_{added}+V_{wet}\varphi))/(V_{wet}\rho_s\ \ (1-\varphi))$ was used, where C^* is the mass of phosphate adsorbed ($\mu mol\ kg^{-1}$), V_{added} is the volume of spiked low-nutrient seawater (ml), V_{wet} is the volume of wet sediment added (ml), φ is the sediment porosity (unitless) and ρ_s is the density of solids ($\rho_s=2.65\ g\ cm^{-3}$; Burdige, 2006). The value of C^* was negative or positive, depending on whether desorption or adsorption had occurred.

A simple linear isotherm, $C^*=KC$, was used to describe the adsorption of phosphate onto solids in the Bering Sea, where C^* is the mass adsorbed per unit mass of total solids (in $\mu mol\ kg^{-1}$), C is the final concentration in solution after 24 h (in μM) and K, the slope of the line, is the linear adsorption coefficient ($L\ kg^{-1}$, the number of moles of phosphorus added to/extracted from the system required to change the phosphate concentration in solution by 1 $mol\ L^{-1}$; Froelich, 1988). A unitless adsorption coefficient (K^*) was calculated by multiplying K by a conversion factor, $\rho_s(1-\varphi)/\varphi$, which is the ratio of weight of sediment solids to volume of pore water ($g\ ml^{-1}$; Krom and Berner, 1980; Slomp et al.,1998).

A buffer diagram was generated for each station by plotting $C_{initial}$ (the amount of dissolved phosphate added, taking into account pore-water phosphate concentrations, in μM) versus ΔC ($C_{initial}-C_{final}$), in μM). The slope of this line indicates the buffering intensity of the sediment. A perfect buffer has a slope of one. Phosphate is usually highly buffered in natural waters, and many sediments display buffer capacities that are near the perfect buffer slope (Froelich, 1988).

2.1.3. Whole–core incubations

Two cores from each station were sub-cored using 8 cm diameter polycarbonate tubing for whole–core incubations. The cores were left uncapped and allowed to temperature equilibrate for 24 h in the dark at near in-situ temperatures (± 2 °C) before being sealed with gas-tight closures equipped with stirrers. Attached to each core was a gravity-fed reservoir of bottom water to replace any bottom water removed during sampling. Phosphate and dissolved oxygen concentrations were measured in a time series of samples from the overlying water over a period of two to seven days. The time series data were fitted to a polynomial and the phosphate and oxygen fluxes (at $t=0$) were calculated using the formula $J=dC/dt|_{t=0}\ VA^{-1}$, where J is the flux (of phosphate or oxygen) in $\mu mol\ m^{-2}\ d^{-1}$, $dC/dt|_{t=0}$ is the instantaneous change in concentration at $t=0$, V is the volume of overlying water in the flux core (m^3) and A is the area of the core (m^2). A negative value for J indicates removal of phosphate or oxygen from the overlying water. Changes in dissolved oxygen over time were measured as the ratio of oxygen to argon using membrane-inlet mass spectrometry (Pfieffer Prisma; Kana et al., 1998). Oxygen fluxes were corrected to account for the addition of reservoir water and to account for slow leakage of oxygen from the silicone caps of the incubation cores. The magnitude of oxygen leakage was determined by comparison of replicate flux cores from 24 stations at which oxygen flux was determined using both silicone (2 cores per station) and PVC caps (2 cores per station). Oxygen fluxes in the silicone capped flux

Please cite this article as: Davenport, E.S., et al., Roles of sorption and tube-dwelling benthos in the cycling of phosphorus in Bering Sea sediments. Deep-Sea Res. II (2012), doi:10.1016/j.dsr2.2012.02.004

cores were corrected using the linear regression equation: corrected flux=1.125*(uncorrected flux)+3.365 (R^2=0.85, n=24).

Phosphate concentrations over time were determined colorimetrically on the SmartChem autoanalyzer as described previously. At the end of the incubation period, all the incubation cores were frozen at −20 °C to preserve the burrow structures for subsequent analysis on shore.

2.2. Laboratory analyses

2.2.1. Burrow abundances

The frozen flux cores were scanned using computed tomography (CT) on a Siemens Sensation 64 CT scanner to determine burrow abundances (Shull and Yasuda, 2001). Although samples were also collected for total benthic infauna, burrow abundances were determined directly because the activities of benthic species in the Bering Sea are not well understood and thus it is expected that burrow abundance will be a better indicator of the effects of benthos on solute flux than infaunal abundances (e.g., Shull et al., 2009; Benoit et al., 2009). The CT scanning generated a series of 2-D axial X-Ray images generated from an X-Ray source rotated around the core. The cores were imaged in 3 mm sections with no overlap and were analyzed using the program ImageJ (National Institutes of Health) to determine the number of burrows in the top section of each incubation core.

2.2.2. Iron determination

Amorphous iron-hydroxides in the freeze-dried sediments from the top 0.5 cm of the incubation cores and from the phosphate adsorption experiments were determined using an ammonium-oxalate extraction (Chao and Zhou, 1983; Phillips and Lovely, 1987; Schulz and Zabel, 2006; Schwertmann, 1973). Extracted iron was measured with a Varian SpectrAA 220FS flame atomic absorption spectrophotometer. Blanks and standards (Inorganic Ventures, 1000 ppm of iron in 1.5% nitric acid) were run for quality control purposes. A calibration standard and blank were run after every 10 samples.

Total iron-oxides in the top 0.5 cm of the incubation cores and the phosphate adsorption experiments were determined by completely dissolving 0.1 g of freeze-dried sediment in Teflon pressure vessels using a Milestone Ethos microwave digestion system. Sediments were digested with trace-metal grade hydrofluoric acid (4 ml) and trace-metal grade nitric acid (12 ml) at 200 °C for 25 min with a 15 min temperature ramp. Samples were diluted to 100 ml using Nanopure water and were analyzed for total iron-hydroxides using atomic absorption spectrophotometry. At least one blank and one standard sediment sample (certified reference marine sediment MESS-3, National Research Council of Canada) were digested with each run of 12 or 24 samples.

2.2.3. Statistical analyses

The data were divided into four of the geographical domains (middle shelf, outer shelf, off shelf and northern Bering shelf) described by Coachman (1986), Lomas et al. (this issue) and Stabeno et al. (this issue). The data from each domain possessed similar pore-water phosphate profiles and sorption isotherms.

Linear regressions were performed on the phosphate flux data from each domain to examine which measured environmental variables (water depth, sediment porosity, sediment oxygen consumption, burrow numbers, amorphous iron hydroxides, total iron-oxides, sediment adsorption coefficients and sediment buffer intensities) contributed most to variation in phosphate fluxes. All linear regressions reported were significant at the α=0.05 level. All statistical analyses were performed using the statistical program R (Free Software Foundation, Inc).

3. Results and discussion

3.1. Bering Sea pore-water profiles

Pore-water profiles can often provide insight into processes affecting the distribution and cycling of phosphate in the sediment. The dissolved phosphate pore-water profiles from the four domains of the Bering Sea suggested different processes were affecting phosphate cycling in each domain. The middle and off shelf pore-water profiles had steep concentration gradients consistent with release of dissolved phosphate from the sediments (Fig. 2A and D). In contrast, the outer and northern Bering shelf profiles possessed low, constant concentrations of dissolved phosphate near the sediment–water interface, which suggested sorption processes were controlling the concentration and subsequent phosphate release (Fig. 2B, C and E).

The steep near-surface concentration gradients in the middle shelf pore-water profiles were consistent with an efflux of phosphorus to the overlying water (Fig. 2A, Table 1). This implies net production of phosphate exceeded the buffering capacity of the sediment (Sundby et al., 1992). The pore-water profiles in the middle shelf domain were also the only profiles to display a decrease in dissolved phosphate with depth below 10 cm at all stations (Fig. 2A), which suggested removal of phosphate at depth. Although not measured directly, this pattern is consistent with the formation and burial of authigenic apatite. Authigenic apatite formation (phosphogenesis) occurs under reducing conditions in the sediment. Highly productive areas or regions with high rates of organic matter sedimentation favor apatite formation, usually continental margins and areas of intense upwelling (Schulz and Zabel, 2006).

The pore-water profiles on the outer shelf displayed two different phosphate distribution patterns. Four of the outer shelf stations displayed almost constant dissolved phosphate concentrations down to 2 cm (Fig. 2B). This region of the sediment may have buffered the concentration of dissolved phosphate in the pore water with excess phosphate adsorbed by amorphous iron-hydroxides and stored in the sediment (Sundby et al., 1992). This process could limit phosphate flux because although organic matter decomposition occurring near the sediment–water interface would result in a direct release of dissolved phosphate to the overlying water, phosphate released to the pore water would be buffered by sorption processes (Slomp et al., 1998). The other two stations did not have a buffering region (Fig. 2C), possibly due to lower rates of net phosphate production. The diffusive fluxes calculated from these profiles were lower than the middle shelf diffusive fluxes (Table 1). The pore-water profiles and diffusive fluxes for the off shelf domain varied widely from station to station (Fig. 2D, Table 1). The depth range for these stations was 600–3500 m and it is possible that different processes were occurring at different depths.

The pore-water profiles and diffusive fluxes from the northern Bering shelf all suggested uptake of dissolved phosphate by the sediments in the top centimeter (negative concentration gradient near the sediment surface), followed by a region of constant dissolved phosphate to 3 cm (Fig. 2E, Table 1). These profiles suggest that these sediments were removing phosphate from the overlying water and accumulating adsorbed phosphate in the sediment. The northern Bering shelf stations had buffering and adsorption capacities similar to the middle shelf, which may have facilitated the uptake of phosphate by these sediments (Table 5). Net phosphate removal at depth was less apparent in these profiles than in the middle shelf profiles. Removal of phosphate might still be occurring, but either at a rate lower than dissolved phosphate production, or at depths greater than 15 cm.

Please cite this article as: Davenport, E.S., et al., Roles of sorption and tube-dwelling benthos in the cycling of phosphorus in Bering Sea sediments. Deep-Sea Res. II (2012), doi:10.1016/j.dsr2.2012.02.004

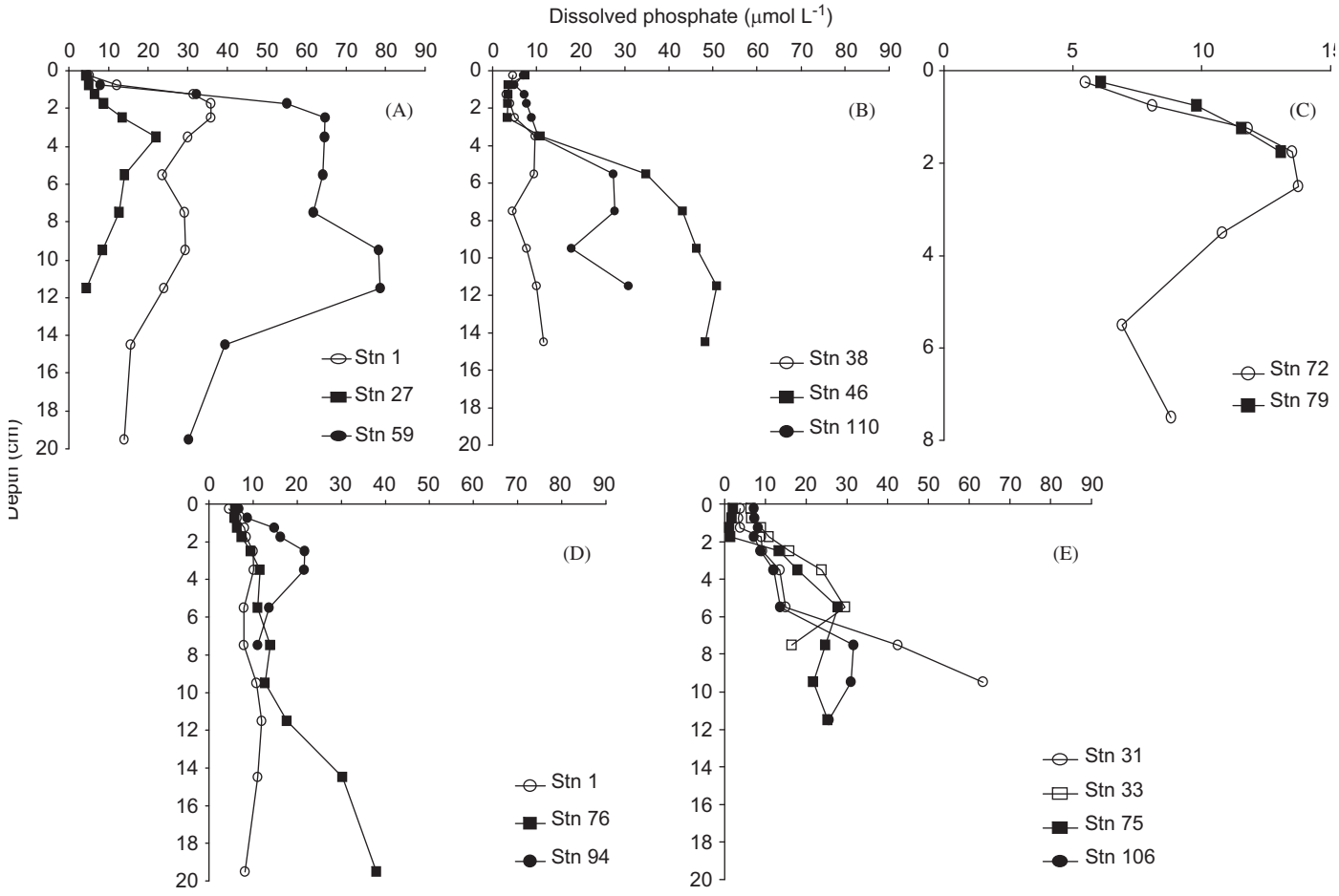

Fig. 2. Pore-water profiles of dissolved phosphate concentrations in cores taken from the different domains of the Bering Sea. (A) Middle shelf at stations 21, 27 and 59. Stations 9 and 62 were not included as there was not enough pore water extracted from these cores to create a profile, (B) Outer shelf, stations that all had profiles with almost constant dissolved phosphate concentrations down to 2 cm, (C) Outer shelf, stations with profiles that had concentration gradients that indicated a release of dissolved phosphate from the sediment. The scale has been changed to show the detail of the profiles, (D) Off shelf, (E) Northern shelf.

3.2. Bering Sea phosphate adsorption

The adsorption of dissolved phosphate onto iron-oxides has been shown to be one of the main regulators of phosphorus cycling in sediments. The four domains of the Bering Sea had very different adsorption and buffering capacities for dissolved phosphate. The sediment adsorption and buffering capacities were high in the shallow-water sediments of the middle and northern Bering Sea domains (Figs. 3 and 4, Tables 2 and 5) suggesting that sorption played an important role in controlling the release of dissolved phosphate from these sediments and helped to maintain low concentrations of pore-water phosphate. Sorption appeared to be less important on the outer and off shelf domains as the phosphate adsorption coefficients and buffering capacities decreased with increasing water depth (Figs. 3 and 4, Tables 3 and 4). Phosphate sorption coefficients for Bering shelf sediments were within the range of values found from other shelf environments. For example, adsorption coefficients were up to forty times higher than values determined for Long Island Sound sediments (Krom and Berner, 1980, 1981) but lower than measured in North Sea sediments (Slomp et al., 1998).

None of the middle shelf stations could be fit with a linear isotherm to determine a unitless adsorption coefficient because essentially all phosphate experimentally added to the pore water was adsorbed by the sediment (Table 2). However, the buffer diagrams generated for the middle shelf stations all had slopes very close to 1 (>0.98), indicating that these sediments were very efficient in adsorbing excess phosphate and maintaining low concentrations of dissolved phosphate in solution (Fig. 4, Table 2; Buffer diagrams could not be generated for stations 9 and 62). Fluxes calculated using the pore water profiles, as well as those measured in the whole–core incubations indicated a large flux of phosphate to the overlying water on the middle shelf (Tables 1 and 2). This suggests that some other process(es) is (are) countering the effects of sorption in these sediments or perhaps phosphate is bypassing the sorptive surface layer in these sediments.

In general, the outer shelf stations had lower buffering capacities than the middle shelf stations, despite similar amorphous iron-hydroxide concentrations (Tables 2 and 3). This suggests that these stations were not as efficient at adsorbing excess phosphate and maintaining constant pore water values at the high levels of phosphate present.

Off the continental shelf, the adsorption coefficients were very low. Station 1 had an adsorption coefficient ($K^*=0.996$) that was lower than that the average adsorption coefficient ($K^*=1.8$) that Krom and Berner (1980, 1981) determined for anoxic Long Island Sound sediments (Fig. 3, Table 4). All of the off shelf stations had low sediment buffering capacities in comparison to the other domains (Fig. 4, Table 4). These sediments were relatively poor at maintaining a constant concentration of dissolved phosphate in the sediment pore water. Phosphate input to these systems would likely overwhelm the buffering capacity and phosphate would not be retained by the sediment. These stations were farthest from

Please cite this article as: Davenport, E.S., et al., Roles of sorption and tube-dwelling benthos in the cycling of phosphorus in Bering Sea sediments. Deep-Sea Res. II (2012), doi:10.1016/j.dsr2.2012.02.004

the coast and at depths of 600 m or deeper. This might have reduced the supply of iron from the water column and from continental weathering. Surface concentrations of iron hydroxides and rates of iron reduction are also lower in these sediments compared to the middle shelf and northern domains (Esch, 2011).

The northern Bering shelf stations had buffering capacities similar to the middle shelf. Station 46 had the highest adsorption coefficient of all the stations for which adsorption coefficients were determined (Tables 2–5). This station also had a high buffering capacity (Fig. 3, Table 5). All stations in the northern Bering shelf had higher phosphate sorption and buffering capacities than stations in the outer and off shelf domains.

3.3. Bering Sea phosphate fluxes

Diffusive fluxes calculated from pore water profiles do not take into account other transport mechanisms, such as bioturbation and bioirrigation. Other studies have shown that the activities of organisms in the sediment have a direct impact on the flux of solutes from the sediment, causing as much as a four fold discrepancy between flux measurements (Berelson et al., 2003; Zabel et al., 1998). If molecular diffusion were the only process occurring in sediments, then the diffusive fluxes and whole core incubation fluxes would be almost identical. This is clearly not the case for all the domains in the Bering Sea (Fig. 5). The middle shelf whole core incubation fluxes had a higher range than the diffusive fluxes, although mean fluxes were similar. The diffusive flux was a close estimate in the off shelf domain, yet underestimated the measured flux in both the outer and northern shelf domains.

If phosphate flux were limited by the supply of phosphorus from organic matter remineralization, then the flux might co-vary with the rate of oxygen consumption. Alternatively, if sorption processes limited the phosphate flux, the flux might be expected to co-vary with iron hydroxide concentration or adsorption coefficients. However, neither of these patterns were evident in the middle shelf. The only independent variable that explained the variation in the phosphate flux in this domain was the number of infaunal burrows found in the top of each incubation core (Fig. 6, Table 2). This variable accounted for 73% of the phosphate flux in the middle shelf domain. It is also important to note that this was the only domain where all of the measured phosphate fluxes were positive. Even though these sediments had high buffering capacities for phosphate, which should maintain low dissolved phosphate pore-water concentrations and limit the flux of phosphate to the overlying water, the measured fluxes indicated a large release of phosphate to the overlying water on the middle shelf (Table 2).

We hypothesize that bioturbation and bioirrigation are the key processes affecting phosphate flux in the middle shelf sediments. In this domain, bioturbation moves iron-hydroxide bound phosphate to the reduced layer of the sediment, where it is then released as the iron-hydroxides undergo reduction (Esch, 2011). Bioturbation could also be responsible for the transport of organic phosphorus to the reduced layer of the sediment, where the concentration profiles suggest phosphate is released or converted to authigenic apatite (Aller, 1994; Burdige, 2006). Bioirrigation leads to an increased exchange of pore water, moving the dissolved phosphate out of the sediment into the overlying water (Aller, 1978). On the middle shelf, infaunal burrows 5 cm in length or longer would have had direct access to high pore-water concentrations of dissolved phosphate. Thus, bioirrigation would bypass the sorptive surficial sediments. These results are consistent with laboratory studies that have shown a significant affect of tube-dwelling benthos on phosphate flux and sorption processes (e.g., Aller, 1978). It is also possible that the presence of benthic organisms on the middle shelf enhances the activities of microbial populations that mediate sedimentary reactions (Aller, 1982). The activities of benthic organisms can stimulate rates of microbially-mediated decomposition reactions by increasing the surface area of organic detritus through feeding, as

Table 1
Diffusive phosphate fluxes calculated from sediment profiles in each domain of the Bering Sea. The sign denotes the direction of the flux (a negative sign indicates a flux of phosphate into the sediment).

Station number	Depth (m)	Diffusive phosphate flux ($\mu mol\ m^{-2}\ d^{-1}$)
Middle shelf		
21	63	28.10
27	100	3.31
59	71	47.10
Outer shelf		
31	143	−1.34
33	143	3.92
72	105	6.70
75	101	4.81
79	120	3.55
106	138	0.70
Off shelf		
1	2608	12.02
76	3437	−0.35
94	600	6.93
Northern shelf		
38	78	−2.07
46	53	−8.35
110	47	−4.81

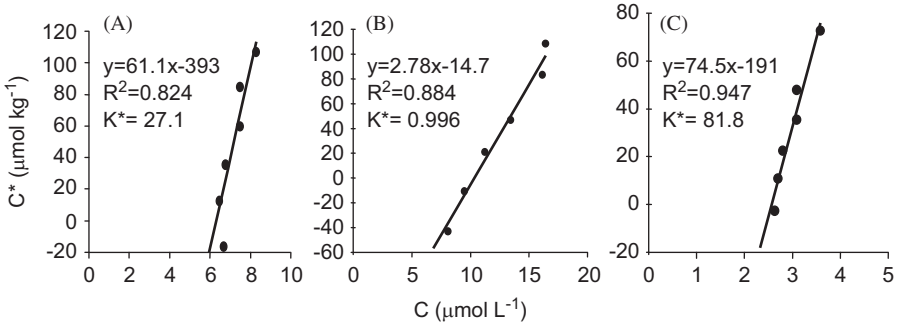

Fig. 3. Examples of adsorption isotherms from the different domains in the Bering Sea for which adsorption isotherms could be generated. (A) Outer shelf station 31, (B) Off shelf station 1, (C) Northern shelf station 46. C^* is the mass of phosphate adsorbed during the experiment and C is the final concentration of dissolved phosphate. The slope of the line is the linear adsorption coefficient, K, which had units of L kg^{-1}. K^* is the unitless adsorption coefficient. All linear regressions are statistically significant at the $\alpha=0.05$ level.

Please cite this article as: Davenport, E.S., et al., Roles of sorption and tube-dwelling benthos in the cycling of phosphorus in Bering Sea sediments. Deep-Sea Res. II (2012), doi:10.1016/j.dsr2.2012.02.004

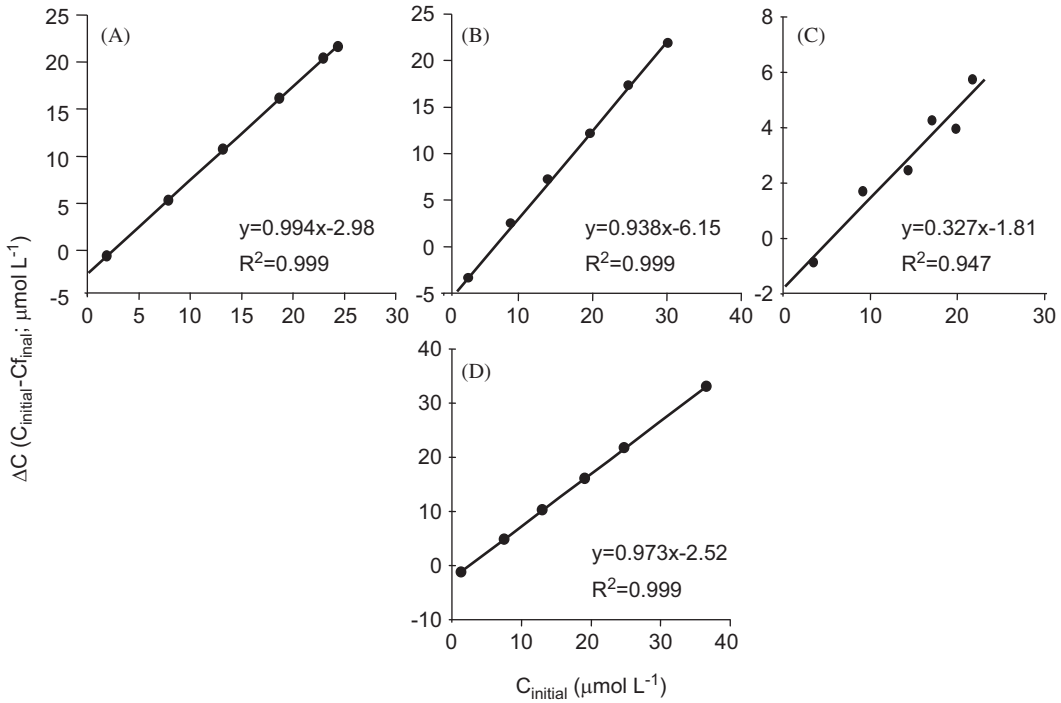

Fig. 4. Examples of buffer diagrams for the different Bering Sea domains. (A) Middle shelf station 27 (B) Outer shelf station 31, (C) Off shelf station 1, (D) Northern shelf station 46. ΔC is the change in phosphate concentration over 24 h. $C_{initial}$ is the initial phosphate concentration added to each tube, taking into account the initial pore-water phosphate concentrations. All linear regressions are statistically significant at the $\alpha = 0.05$ level.

Table 2
A summary of the sediment properties measured in each sediment core from the middle shelf stations. Letters indicate replicates. Data that were missing or not available for the replicate at each station were indicated.

Station	Depth (m)	Top 0.5 cm sediment porosity (unitless)	Phosphate flux (whole–core incubations, μmol m^{-2} d^{-1})	Sediment oxygen consumption (whole–core incubations, μmol m^{-2} d^{-1})	Burrow numbers (per 50 cm^2 core)	Top 0.5 cm amorphous iron-hydroxides (μmol g^{-1})	Top 0.5 cm dissolved phosphate (μM)	Slope of adsorption isotherm (K; L kg^{-1})	Unitless adsorption coefficient (K^*)	Sediment buffer intensity (unitless)
9a	67	0.54	26.92	−7401.69	16	89.37	–	–	–	–
9b	67	0.54	1.05	−3933.44	13	87.74	–	–	–	–
21a	63	0.81	37.74	−5068.96	21	142.24	6.40	–	–	0.98
21b	63	0.81	84.75	−6420.05	32	183.55	5.09	–	–	–
27a	100	0.86	1.19	−6333.50	11	164.24	1.55	–	–	0.99
27b	100	0.86	2.58	−5139.23	11	138.99	4.34	–	–	–
59a	71	0.85	11.46	−4690.71	11	169.55	4.83	–	–	1.01
59b	71	0.85	12.18	−5630.87	23	170.60	4.79	–	–	–
62a	67	–	45.93	−5810.18	24	99.15	–	–	–	–
62b	67	–	20.74	−5475.78	10	87.08	–	–	–	–

Table 3
A summary of the sediment properties measured in each sediment core from the outer shelf stations. Letters indicate replicates. Data that were missing or not available for the replicate at each station were indicated.

Station	Depth (m)	Top 0.5 cm sediment porosity (unitless)	Phosphate flux (whole–core incubations, μmol m^{-2} d^{-1})	Sediment oxygen consumption (whole–core incubations, μmol m^{-2} d^{-1})	Burrow numbers (per 50 cm^2 core)	Top 0.5 cm amorphous iron-hydroxides (μmol g^{-1})	Top 0.5 cm dissolved phosphate (μM)	Slope of adsorption isotherm (K; L kg^{-1})	Unitless adsorption coefficient (K^*)	Sediment buffer intensity (unitless)
31a	143	0.90	11.76	−7075.63	8	169.76	3.77	61.10	27.10	0.94
31b	143	0.90	32.49	−6728.60	14	140.10	4.77	–	–	–
33a	143	0.81	17.74	−4097.54	3	91.32	6.50	–	–	0.93
33b	143	0.81	16.73	−4755.53	13	77.96	6.62	–	–	–
72a	105	0.74	5.46	−4166.96	11	66.33	6.40	14.60	17.90	0.90
72b	105	0.74	14.37	−4086.02	5	68.90	5.49	–	–	–
75	101	0.79	−19.37	−4818.37	9	119.93	2.02	7.69	7.78	0.83
79	120	0.59	16.42	−4045.16	2	52.83	7.26	3.10	6.59	0.77
106a	138	0.84	19.74	−5255.52	–	84.43	7.16	–	–	1.02
106b	138	0.84	26.77	−4421.26	3	85.09	6.08	–	–	–

Please cite this article as: Davenport, E.S., et al., Roles of sorption and tube-dwelling benthos in the cycling of phosphorus in Bering Sea sediments. Deep-Sea Res. II (2012), doi:10.1016/j.dsr2.2012.02.004

Table 4
A summary of the sediment properties measured in each sediment core from the off shelf stations. Cores from stations 1 and 76 were not kept at in-situ pressures and as a result there may be some pressure effects on the pore-water chemistry of these cores (Ferdelman et al., 1999). Letters indicate replicates. Data that were missing or not available for the replicate at each station were indicated.

Station	Depth (m)	Top 0.5 cm sediment porosity (unitless)	Phosphate flux (whole–core incubations, μmol m^{-2} d^{-1})	Sediment oxygen consumption (whole–core incubations, μmol m^{-2} d^{-1})	Burrow numbers (per 50 cm^2 core)	Top 0.5 cm amorphous iron-hydroxides (μmol g^{-1})	Top 0.5 cm dissolved phosphate (μM)	Slope of adsorption isotherm (K; L kg^{-1})	Unitless adsorption coefficient (K^*)	Sediment buffer intensity (unitless)
1a	2608	0.90	−9.02	−2785.34	16	77.94	5.25	2.78	0.99	0.33
1b	2608	0.90	5.10	−2792.97	8	105.40	4.49	–	–	–
76a	3437	0.95	67.33	−2968.69	17	83.23	5.77	16.30	3.92	0.66
76b	3437	0.95	4.10	−3764.74	24	120.01	5.97	–	–	–
94a	600	0.70	2.09	−3785.49	10	34.44	6.30	3.16	4.47	0.65

Table 5
A summary of the sediment properties measured in each sediment core from the northern shelf stations. Letters indicate replicates. Data that were missing or not available for the replicate at each station were indicated.

Station	Depth (m)	Top 0.5 cm sediment porosity (unitless)	Phosphate flux (whole–core incubations, μmol m^{-2} d^{-1})	Sediment oxygen consumption (whole–core incubations, μmol m^{-2} d^{-1})	Burrow numbers (per 50 cm^2 core)	Top 0.5 cm amorphous iron-hydroxides (μmol g^{-1})	Top 0.5 cm dissolved phosphate (μM)	Slope of adsorption isotherm (K; L kg^{-1})	Unitless adsorption coefficient (K^*)	Sediment buffer intensity (unitless)
38a	78	0.84	10.26	−5655.18	24	125.59	5.48	9.81	7.75	0.78
38b	78	0.84	5.53	−4776.21	6	139.65	4.57	–	–	–
46a	53	0.74	4.12	−4226.30	20	107.60	5.67	74.50	81.81	0.97
46b	53	0.74	5.52	−4303.00	18	94.86	7.42	–	–	–
110a	47	0.72	53.66	−10890.43	15	94.83	9.44	–	–	1.01
110b	47	0.72	−18.40	−7196.87	10	93.79	6.94	–	–	–

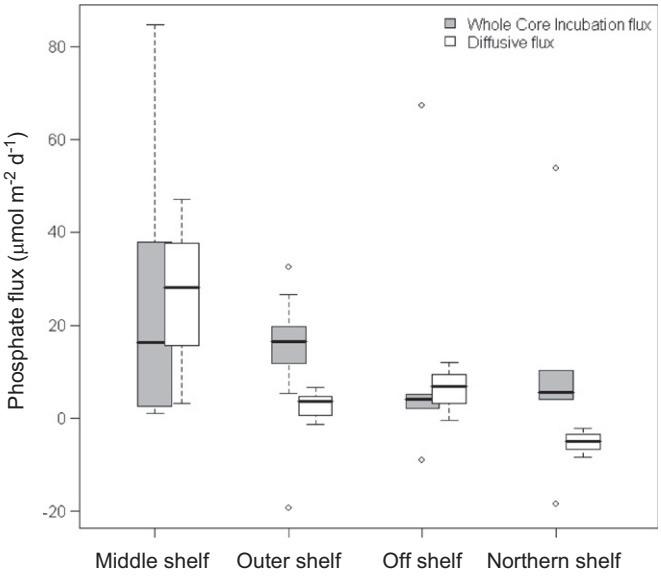

Fig. 5. Box and whisker plots showing both diffusive and whole core incubation fluxes calculated for each domain of the Bering Sea. The box represents the 25–75% range of the data (lower and upper quartiles, respectively). The horizontal band represents the median. The whiskers represent data that are within 1.5 interquartile range (IQR) of the lower or upper quartiles. Outliers (beyond 1.5 IQR) are denoted by open circles.

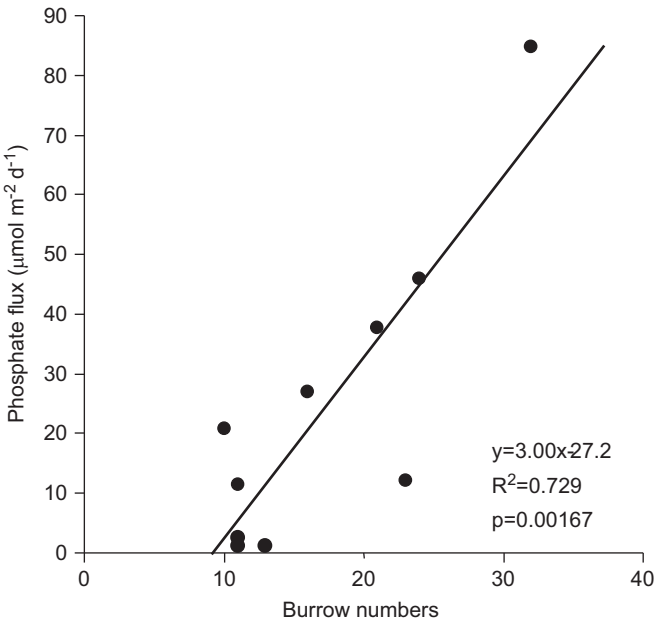

Fig. 6. Regression between phosphate flux (whole–core incubations) and the number of burrows found in the top of each incubation core on the middle shelf. The least-squares relationship and model I linear regression statistics are shown.

well as grazing microbial populations, effectively keeping them in a high-productivity phase (Aller, 1982) and thus enhancing the flux of dissolved phosphate to the overlying water.

The outer shelf has annual rates of net primary productivity similar to that of the middle shelf (43–59 Tg yr^{-1} and 47–49 Tg C yr^{-1}, respectively; Lomas et al., this issue), yet burrow numbers were not nearly as high and burrow abundance was not correlated with phosphate flux in this domain. A significant negative relationship was observed between amorphous iron-hydroxide and dissolved phosphate concentrations in the top 0.5 cm of the sediment column (Fig. 7) that suggested iron-hydroxides could have played a role in limiting the concentration of dissolved phosphate in the upper region of the sediment. None

Please cite this article as: Davenport, E.S., et al., Roles of sorption and tube-dwelling benthos in the cycling of phosphorus in Bering Sea sediments. Deep-Sea Res. II (2012), doi:10.1016/j.dsr2.2012.02.004

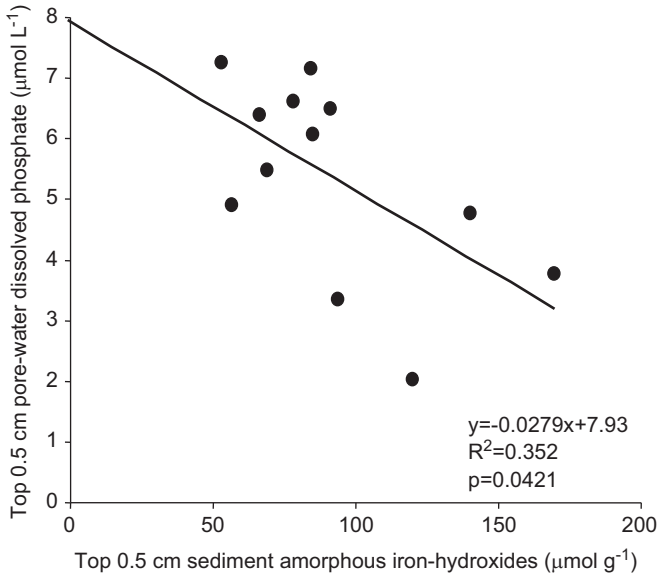

Fig. 7. Regression between dissolved phosphate concentrations in the top 0.5 cm of the sediment and amorphous iron-hydroxide concentrations in the top 0.5 cm of the sediment on the outer shelf. The least-squares relationship and model I linear regression statistics are shown.

of the environmental factors we measured could adequately explain the phosphate flux in this domain. Due to the structuring of the outer shelf front, there is a weakened cross-shelf circulation between the outer and middle shelf domains. This constrains zooplankton biomass to the outer shelf and they consume more of the primary production in the water column, rather than allowing the organic matter to reach the sediment as it does in the middle shelf domain (Coyle et al., 2008; Moran et al., this issue). Consequently, organic matter deposited on the outer shelf may provide less food for benthic organisms, supporting lower populations than the middle shelf.

Phosphate fluxes in the off shelf domain were lower than fluxes measured on the shelf (Table 4). The phosphate fluxes measured in the northern Bering Sea were similar in magnitude to those measured in other domains of the Bering shelf (Table 5). However, the phosphate flux in both of these domains was not significantly correlated with any of the measured environmental variables. Molecular diffusion is likely the dominant transport process affecting the flux in the off shelf domain. Depths of 600 m or greater would support lower abundances of organisms compared to shallower areas such as the middle shelf (Tables 2–4).

3.4. Implications for a changing Bering Sea

The pore-water profiles point toward different processes controlling the dissolved phosphate concentrations in different domains of the Bering Sea. By the same token, the effects of climate change on the Bering Sea might not be the same in each domain. Earlier ice-melt due to a warming climate could cause an ecosystem regime change (Hunt et al., 2002; Grebmeier et al., 2006; Stabeno et al., this issue). Organisms that currently reside in one domain of the Bering Sea may move to another domain, changing food chain dynamics (Stabeno et al., this issue). Domains that show tight coupling between primary production and benthic communities (like the northern Bering shelf) may transition into ecosystems where more of the primary production fuels the pelagic ecosystem. Past regime changes (1976–1977) have been shown to increase epibenthic biomass and re-structure epibenthic communities in several domains of the Bering Sea (Conners et al., 2002; Hamazaki et al., 2005). Changes in food availability and bottom water temperatures could also impact benthic infaunal species diversity and abundance, which can affect phosphate exchange (Waldbusser et al., 2004).

A change in the timing of the spring bloom could have numerous consequences for benthic infauna and nutrient cycling in Bering Sea shelf sediments. Our results point toward one potential impact. We predict that long-term changes in infaunal abundance would influence rates of bioirrigation and thus phosphate cycling. If benthic infaunal abundances were to decrease on the middle shelf as observed on the northern shelf (Grebmeier et al., 2006), we would expect sorption to become a much more important process and thus reducing the sedimentary phosphate flux. On the other hand, if the abundance of burrow-dwelling benthos in this domain were to increase, we would expect enhanced flux of phosphate via burrow irrigation, which bypasses sorptive surficial sediments. The permanent storage of phosphate occurring on the middle shelf could also be impacted by changes in benthic biomass and rates of bioturbation (Slomp et al., 1996).

Controls on the phosphate flux on the middle shelf cannot be properly understood unless benthic infaunal abundance is taken into account. Measurements of sediment oxygen consumption and sorption to iron-hydroxides alone are not adequate to describe the processes affecting phosphorus cycling, because infaunal burrows appear to bypass the sorptive layer of amorphous iron-hydroxides near the sediment surface and directly connect high concentrations of dissolved phosphate at depth with the overlying water.

Acknowledgments

We thank the captain and crew of the USCG Healy for all their help and support, the coring team at Oregon State University who made sure the coring operations ran smoothly, Heather Whitney of UW for help with sample collection, as well as Calvin Mordy of JISAO/NOAA/UW and Erin Macri of WWU for help with sample analysis. This research was funded by National Science Foundation grants ARC0612380 and MRI0723234 to David Shull and ARC0612436 to Allan Devol as part of the Bering Ecosystem Study. This is BEST-BSIERP contribution number 48.

References

Aguilar-Islas, A.M., Rember, R.D., Mordy, C.W., Wu, J., 2008. Sea ice-derived dissolved iron and its potential influence on the spring algal bloom in the Bering Sea. Geophys. Res. Lett. 35 (L24601), 5 pp.

Aller, R.C., 1978. Experimental studies of changes produced by deposit feeders on pore-water, sediment and overlying water chemistry. Am. J. Sci. 278, 1185–1234.

Aller, R.C., 1982. The effects of macrobenthos on chemical properties of marine sediment and overlying water. In: McCall, P.L., Tevesz, M.J.S. (Eds.), Animal–Sediment Relations. Plenum Press, New York.

Aller, R.C., 1994. Bioturbation and remineralization of sedimentary organic matter: effects of redox oscillation. Chem. Geol. 114, 331–345.

Anschutz, P., Shaojun, Z., Sundby, B., Mucci, A., Gobeil, C., 1998. Burial efficiency of phosphorous and the geochemistry of iron in continental margin sediments. Limnol. Oceanogr. 43, 53–64.

Benoit, J.A., Shull, D.H., Harvey, R.M., Beal, S.A., 2009. Effect of bioirrigation on sediment–water exchange of methylmercury in Boston Harbor, Massachusetts. Environ. Sci. Technol. 43, 3669–3674.

Berelson, W., McManus, J., Coale, K., Johnson, K., Burdige, D., Kilgore, T., Colodner, D., Chavez, F., Kudela, R., Boucher, J., 2003. A time series of benthic flux measurements from Monterey Bay, CA. Cont. Shelf Res. 23, 457–481.

Boudreau, B.P., 1997. Diagenetic models and their implementation: modeling transport and reactions in aquatic sediments. Springer-Verlag, Berlin Heidelberg 414 pp.

Burdige, D.J., 2006. Geochemistry of marine sediments. Princeton University Press, New Jersey 630 pp.

Chao, T.T., Zhou, L., 1983. Extraction techniques for selective dissolution of amorphous iron oxides from soils and sediments. Soil Science Society of America Journal 47, 225–232.

Coachman, L.K., 1986. Circulation, water masses, and fluxes on the southeastern Bering Sea shelf. Cont. Shelf Res. 5, 23–108.

Conners, M.E., Hollowed, A.B., Brown, E., 2002. Retrospective analysis of Bering Sea bottom trawl surveys: regime shift and ecosystem reorganization. Prog. Oceanogr. 55, 209–222.
Coyle, K.O., Pinchuk, A.I., Eisner, L.B., Napp, J.M., 2008. Zooplankton species composition, abundance and biomass on the Eastern Bering Sea shelf during summer: The potential role of water-column stability and nutrients in structuring the zooplankton community. Deep-Sea Res. II: 55, 1775–1791.
Esch, M.E.S., 2011. Iron and Manganese Reduction in Bering Sea Shelf Sediments. Master's Thesis, Western Washington University, Bellingham. 69 pp.
Ferdelman, T.G., Fossing, H., Neumann, K., 1999. Sulfate reduction in surface sediments of the southeast Atlantic continental margin between 15°38′S and 27°57′S (Angola and Namibia). Limnol. Oceanogr. 44, 650–661.
Froelich, P.N., 1988. Kinetic control of dissolved phosphate in natural rivers and estuaries: a primer on the phosphate buffer mechanism. Limnol. Oceanogr. 33, 649–668.
Goering, J.J., Iverson, R.L., 1981. Phytoplankton distribution on the southeastern Bering Sea shelf. In: Hood, D.W., Calder, J.A. (Eds.), The Eastern Bering Sea Shelf: Oceanography and Resources (2). Juneau, NOAA, pp. 933–946.
Grebmeier, J.M., Overland, J.E., Moore, S.E., Farley, E.V., Carmack, E.C., Cooper, L.W., Frey, K.E., Helle, J.H., McLaughlin, F.A., McNutt, S.L., 2006. A major ecosystem shift in the northern Bering Sea. Science 311, 1461–1463.
Hamazaki, T., Fair, L., Watson, L., Brennan, E., 2005. Analyses of Bering Sea bottom-trawl surveys in Norton Sound: absence of regime shift effect on epifauna and demersal fish. ICES Journal of Marine Science 62, 1597–1602.
Hunt, G.L., Stabeno, P., Walters, G., Sinclair, E., Brodeur, R.D., Napp, J.M., Bond, N.A., 2002. Climate change and control of the southeastern Bering Sea pelagic ecosystem. Deep-Sea Res. II 49, 5821–5853.
Kana, T.M., Sullivan, M.B., Cornwell, J.C., Groszkowske, K.M., 1998. Denitrification in estuarine sediments determined by membrane inlet mass spectrometry. Limnol. Oceanogr. 43, 334–339.
Krom, M.D., Berner, R.A., 1980. Adsorption of phosphate in anoxic marine sediments. Limnol. Oceanogr. 25, 797–806.
Krom, M.D., Berner, R.A., 1981. The diagenesis of phosphorus in nearshore marine sediment. Geochim. Cosmochim. Acta 45, 207–216.
Lehmann, M.F., Sigman, D.M., McCorkle, D.C., Brunelle, B.G., Hoffmann, S., Kienast, M., Cane, G., Clement, J., 2005. Origin of the deep Bering Sea nitrate deficit: constraints from the nitrogen and oxygen isotopic composition of water column nitrate and benthic nitrate fluxes. Global Biogeochem. Cycles 19, GB4005. doi:10.1029/2005GB002508.
Lomas, M.W., Moran, S.B., Casey, J.R., Bell, D.W., Tiahlo, M., Whitefield, J., Kelly, R.P., Mathis, J.T., Cokelet, E.D. Spatial and seasonal variability of primary production on the eastern Bering Sea shelf. Deep-Sea Res. II, this issue [doi:10.1016/j.dsr2.2012.02.010].
McManus, J., Berrelson, W.M., Coale, K.H., Johnson, K.S., Kilgore, T.E., 1997. Phosphorus regeneration in continental margin sediments. Geochim. Cosmochim. Acta 61, 2891–2907.
Moran, S.B., Lomas, M.W., Kelly, R.P., Gradinger, R., Iken, K., Mathis, J.T. Seasonal succession of net primary productivity, particulate organic carbon export, and autotrophic community composition in the eastern Bering Sea. Deep-Sea Res. II, this issue [doi:10.1016/j.dsr2.2012.02.011].
Mordy, C.W., Stabeno, P.J., Ladd, C., Zeeman, S., Wisegarver, D.P., Salo, S.A., Hunt, G.L., 2005. Nutrients and primary production along the eastern Aleutian island archipelago. Fish. Oceanogr. 14, 55–76.
Palenik, B., Dyhrman, S.T., 1998. Recent progress in understanding the regulation of marine primary production by phosphorus. In: Lynch, J.P., Diekman, J. (Eds.), Phosphorus in Plant Biology: Regulating Roles in Molecular, Cellular, Organismic and Ecosystem Processes. American Society of Plant Physiologists, Rockville, Md, pp. 26–38.
Phillips, E.J.P., Lovely, D.R., 1987. Determination of Fe(III) and Fe(II) in oxalate extracts of sediment. Soil Sci. Soc. Am. J. 51, 938–941.
Redfield, A.C., 1958. The biological control of chemical factors in the environment. Am. Sci. 46, 205–222.
Rozan, T.F., Herszage, J., Valdes, L.M., Price, K.S., Luther III, G.W., 2002. Iron-sulfur-phosphorus cycling in the sediments of a shallow coastal bay: implications for sediment nutrient release and benthic macroalgal blooms. Limnol. Oceanogr. 47, 1346–1354.
Schlesinger, W.H., 2004. Biogeochemistry: A Treatise on Geochemistry, Vol. 8. Elsevier Inc., San Diego 720 pp.
Schlitzer, R., 2008. Ocean Data View 〈http://odv.awi.de〉.
Schulz, H.D., Zabel, M., 2006. Marine Geochemistry, 2nd ed. Springer, Berlin Heidelberg, New York 574 pp.
Schumacher, J.D., Kinder, T.J., Pashinski, D.J., Charnell, R.L., 1979. A structural front over the continental shelf of the eastern Bering Sea. J. Phys. Oceanogr. 9, 79–87.
Schwertmann, U., 1973. Use of oxalate for Fe extraction from soils. Can. J. Soil Sci. 53, 244–246.
Shull, D.H., Yasuda, M., 2001. Size-selective downward particle transport by cirratulid polychaetes. J. Mar. Res. 59, 453–473.
Shull, D.H., Benoit, J.M., Wojcik, C., Senning, J.R., 2009. Infaunal burrow ventilation and pore-water transport in muddy sediments. Estuarine Coastal Shelf Sci. 83, 277–286.
Slomp, C.P., Epping, E.H.G., Helder, W., Van Raaphorst, W., 1996. A key role for iron-bound phosphorus in authigenic apatite formation in North Atlantic continental platform sediments. J. Mar. Res. 54, 1179–1205.
Slomp, C.P., Malchaert, J.F.P., Van Raaphorst, W., 1998. The role of adsorption in sediment–water exchange of phosphate in North Sea continental margin sediments. Limnol. Oceanogr. 43, 832–846.
Springer, A.M., McRoy, C.P., Flint, M.V., 1996. The Bering Sea green belt: shelf-edge processes and ecosystem production. Fish. Oceanogr. 5, 205–223.
Stabeno, P.J., Bond, N.A., Kachel, N.B., Salo, S.A., Schumacher, J.D., 2001. On the temporal variability of the physical environment of the southeastern Bering Sea. Fish. Oceanogr. 10, 81–98.
Stabeno, P.J., Farley, E., Kachel, N.B., Moore, S., Mordy, C., Napp, J.M., Overland, J.E., Pinchuk, A.I., Sigler, M. A comparison of the physics of the northern and southern shelves of the eastern Bering Sea and some implications for the ecosystem. Deep-Sea Res. II, this issue [doi:10.1016/j.dsr2.2012.02.019].
Sundby, B., Gobiel, C., Silverberg, N., Mucci, A., 1992. The phosphorous cycle in coastal marine sediments. Limnol. Oceanogr. 37, 1129–1145.
Tanaka, T., Laodong, G., Deal, C., Tanaka, N., Whiteledge, T., Murata, A., 2004. N deficiency in a well-oxygenated cold bottom water over the Bering Sea shelf: influence of sedimentary denitrification. Cont. Shelf Res. 24, 1271–1283.
Tyrrell, T., 1999. The relative influences of nitrogen and phosphorus on oceanic primary productivity. Nature 400, 525–531.
Van Capellen, P., Ingall, E.D., 1994. Benthic phosphorus regeneration, net primary production, and ocean anoxia: a model of the coupled marine biogeochemical cycles of carbon and phosphorus. Paleooceanography 9, 677–692.
Waldbusser, G.G., Marinelli, R.L., Whitlach, R.B., Visscher, P.T., 2004. The effects of infaunal biodiversity on biogeochemistry of coastal marine sediments. Limnol. Oceanogr. 49, 1482–1492.
Zabel, M., Dahmke, A., Schulz, H.D., 1998. Regional distribution of diffusive phosphate and silicate fluxes through the sediment–water interface: the eastern South Atlantic. Deep-Sea Res. I 45, 277–300.

Please cite this article as: Davenport, E.S., et al., Roles of sorption and tube-dwelling benthos in the cycling of phosphorus in Bering Sea sediments. Deep-Sea Res. II (2012), doi:10.1016/j.dsr2.2012.02.004